Published in final edited form as:

Bioorg Med Chem Lett. 2016 August 01; 26(15): 3603–3607. doi:10.1016/j.bmcl.2016.06.010.

Discovery of *N*-(3-fluoro-4-methylsulfonamidomethylphenyl)urea as a potent TRPV1 antagonistic template

Jihyae Ann[a,†], **Wei Sun**[b,†], **Xing Zhou**[c], **Aeran Jung**[a], **Jisoo Baek**[a], **Sunho Lee**[a], **Changhoon Kim**[a], **Suyoung Yoon**[a], **Sunhye Hong**[d], **Sun Choi**[d], **Noe A. Turcios**[e], **Brienna K. A. Herold**[e], **Timothy E. Esch**[e], **Nancy E. Lewin**[e], **Adelle Abramovitz**[e], **Larry V. Pearce**[e], **Peter M. Blumberg**[e], **Jeewoo Lee**[a,*]

[a]Laboratory of Medicinal Chemistry, Research Institute of Pharmaceutical Sciences, College of Pharmacy, Seoul National University, Seoul 151-742, Republic of Korea

[b]Shenyang Pharmaceutical University, Shenyang 110016, China

[c]Hainan Institute of Materia Medica, Haikou 570311, China

[d]National Leading Research Laboratory of Molecular Modeling & Drug Design, College of Pharmacy, Graduate School of Pharmaceutical Sciences, Ewha Womans University, Seoul 120-750, Republic of Korea

[e]Laboratory of Cancer Biology and Genetics, Center for Cancer Research, National Cancer Institute, NIH, Bethesda, MD 20892, USA

Abstract

A series of homologous analogues of prototype antagonist **1** and its urea surrogate were investigated as *h*TRPV1 ligands. Through one-carbon elongation in the respective pharmacophoric regions, *N*-(3-fluoro-4-methylsulfonamidomethylphenyl)urea was identified as a novel and potent TRPV1 antagonistic template. Its representative compound **27** showed a potency comparable to that of lead compound **1**. Docking analysis of compound **27** in our *h*TRPV1 homology model indicated that its binding mode was similar with that of **1*S***.

Keywords

Vanilloid receptor 1; TRPV1 antagonists; Analgesic

TRPV1 has emerged as a promising novel therapeutic target for the management of chronic and inflammatory pain.[1–3] Building on initial insights provided by the prototypic ligands for TRPV1, capsaicin[4] and resiniferatoxin,[5] our understanding of the structure activity requirements for antagonistic ligands is maturing.[6,7] Solution of the structure of TRPV1 by cryo electron microscopy[8,9] and insights yielded by modeling[10,11] provide a powerful complement guiding and validating the development of lead therapeutic structures.

*Corresponding author. Tel.: +82 2 880 7846; fax: +82 2 762 8322. jeewoo@snu.ac.kr (J. Lee).

†These two authors contributed equally to this work.

Over the last years, we have demonstrated that a series of 2-(3-fluoro-4-methylsulfonamidophenyl)propanamides were potent *h*TRPV1 antagonists active against multiple activators.[12–19] Their structure activity relationship has been investigated extensively based on the three pharmacophoric regions, designated the A-, B-, and C-regions. In these investigations, compound **1** was identified as a prototype antagonist, possessing 3-fluoro-4-methyl-sulfonamidophenyl in the A-region, propanamide in the B-region, and (6-trifluoromethyl-pyridin-3-yl)methyl in the C-region (Fig. 1).[12] Compound **1** exhibited highly potent and (*S*)-stereospecific antagonism of *h*TRPV1 activators including capsaicin, low pH, heat (45 °C) and *N*-arachidonoyl dopamine (NADA). Recently we reported that the α-*m*-tolyl congener **2** showed high potency and selective antagonism of capsaicin with a 3-fold improvement over prototype **1**.[18] Molecular modeling using our established *h*TRPV1 homology model indicated that the enhanced potency of **2** might be attributed to additional specific hydrophobic interactions of the *m*-tolyl group with the receptor.

In continuation of our program to discover novel antagonistic templates with the goal of developing clinical candidates for TRPV1 mediated neuropathic pain, we have investigated a series of one carbon homologated analogues of prototype antagonist **1** and its urea B-region surrogate **21** (Fig. 1). This homologation approach can provide the optimal orientation of the three pharmacophoric region by varying their positions. Of particular interest, the urea B-region surrogates have an advantage over the corresponding propanamide B-region antagonists previously reported[12–19] in terms of synthetic accessibility because the urea is achiral, unlike the chiral propanamide, and the A-region amines, precursors for urea coupling, are more commercially accessible.

In this study, we synthesized one-carbon elongated analogues in the respective A-, B-, C-regions and evaluated their binding affinities and antagonism of *h*TRPV1 activation by capsaicin. With the optimized potent antagonistic template, we performed a docking study using our *h*TRPV1 homology model to analyze its binding interactions with the receptor.

The syntheses of the C-region intermediates for coupling with the A-region are shown in Scheme 1. The C-region amine **4** and its *N*-trichloroacetyl derivative **5** were prepared from the nitrile **3** as previously reported.[12]

The one-carbon elongated analogue of **4** was also prepared from **3** by the conventional 5-step route. For the synthesis of the one-carbon elongated C-region analogue of **1**, the propionic acid **9**[12] was converted to the corresponding pentafluorophenyl ester which reacted with the amine **8** to provide **11** (Scheme 2).

For the synthesis of the one-carbon elongated A-region analogue of **1**, the commercially available amine **12** was mesylated and its bromide was substituted with ethyl propionate by a nickel-catalyzed cross-coupling reaction[20] to afford **14**, which was hydrolyzed and then coupled with the amine **4** to provide **16** (Scheme 3).

The B-region urea surrogate of **1** and its one-carbon elongated C-region analogue, **21** and **22**, respectively, were synthesized by the coupling between the C-region amines and the

phenylcarbamate **20**, which was prepared from the commercially available amine **17** by the conventional 3 steps (Scheme 4).

For the synthesis of the one-carbon elongated A-region analogue of **21**, the methyl group of commercially available **23** was converted in 3 steps to the corresponding amine **24**, which was mesylated and then hydrogenated to give **25**. The carbamoylation of **25** followed by coupling with amine **4** produced **27** (Scheme 5).

For the synthesis of one-carbon elongated B-region analogues of **21**, the commercially available amine **28** was mesylated and its iodo group was converted in 2 steps to the corresponding benzyl amine **30**, followed by coupling with the amine **2** to provide **31**. On the other hand, the propionic acid **9** underwent Curtius rearrangement and subsequent addition with the amine **4** afforded α-methyl analogue of **31** (Scheme 6).

For the synthesis of the one-carbon elongated A and B-region analog of **21**, the bromide **13** was converted to the corresponding nitrile **33**, which was reduced and then coupled with the trichloroacetamide **5** to provide **34** (Scheme 7).

Finally, the commercially available amine **35** was methylated in 3 steps to give **37**. Similarly, the bromide **36** was substituted with a *m*-tolyl group by Buchwald–Hartwig amination to give **38**. The carbamoylation of **37** and **38** followed by coupling with the amine 4 provided the adducts **39** and **40**, which were reduced and then mesylated to produce **41** and **42**, the *N*-methyl and *N*-m-tolyl analogues, respectively, of **21** (Scheme 8).

The binding affinities and potencies as agonists/antagonists of the synthesized TRPV1 ligands were assessed in vitro by a binding competition assay with [^{3}H]-resiniferatoxin (RTX) and by a functional $^{45}Ca^{2+}$ uptake assay using human TRPV1 heterologously expressed in Chinese hamster ovary (CHO) cells, as previously described.[21] For the agonism assay, a saturating concentration of capsaicin (1 μM) was used to define maximal response. For the antagonism assay, the dose-dependent inhibition of the capsaicin (30 nM) stimulated calcium uptake was measured. The K_i values for antagonism take into account the competition between capsaicin and the antagonist. The results are summarized in Table 1, together with the potencies of previous lead compounds **1** and **1*S***.

Prototype **1**, identified from previous analysis of SAR, possessed its four principal pharmacophores including methylsulfonamide in the A region, propanamide in the B-region, and trifluoromethyl and 4-methylpiperidinyl groups in the C-region. Docking analysis with *h*TRPV1 revealed that hydrogen bonding and a π-π interaction with Tyr511 and hydrophobic interactions with the two pockets composed of Met514/Leu515 and Leu547/Thr550 were critical for activity (Fig. 2).

In order to identify whether the pharmacophores in **1** are positioned at optimal distances from one another, we investigated the two one-carbon elongated analogues of **1**, viz. **11** and **16**. Compound **11**, the one-carbon elongated analogue in the C-region, showed 7-fold and 43-fold weaker binding affinity and antagonistic potency, respectively, compared to **1**. Compound **16**, the one-carbon elongated analogue in the A-region, exhibited 29-fold and **12**-fold weaker binding affinity and antagonistic potency, respectively. The results indicated that

prototype **1** possessed an optimal interval between the key pharmacophores in the propanamide B-region series.

Next, we explored the corresponding series of urea B-region analogues with one-carbon homologation. The urea surrogate of **1** was examined first. Surprisingly, substitution of propanamide in **1** with the isosteric urea, providing **21**, led to a dramatic reduction in activity, with 11-fold and 67-fold decreases in binding affinity and antagonism, respectively, compared to **1**. These results suggested that conformational restriction in the urea B-region may affect the positions of the pharmacophores in the A- and C-region, shifting them away from the bioactive conformation. To explore this issue further, we examined one-carbon elongated analogues of **21** in the respective A- and C-regions. Whereas the one-carbon elongated analogue **22** in the C-region proved to be a partial antagonist, the one-carbon elongated analogue **27** in the A-region showed a dramatic improvement in activity with K_i = 6.77 nM and $K_{i(ant)}$ = 12.5 nM, representing approximately 12-fold increases in binding affinity and antagonistic potency compared to **21**. The binding potency of **27** is comparable to that of **1**, indicating that compound **27** as a urea B-region antagonist proved to be a novel antagonistic template with high potency. We also examined the homologated analogues in the urea B-region. The one-carbon elongated analogue **31** displayed a moderate increase in potency compared to **21**. Its α-methyl surrogate **32** showed activity comparable to that of **31**. However, one-carbon elongation in both the A- and B-regions, providing **34**, caused a large decline in activity.

Previous SAR study in a series of α-substituted acetamide B-region derivatives demonstrated that the α-m-tolyl derivative **2** showed highly potent and selective antagonism of capsaicin with a 3-fold improvement in potency over the corresponding α-methyl derivative **1**, probably due to a specific hydrophobic interaction of the *m*-tolyl group with *h*TRPV1.[20]

Accordingly, we explored the *N*-methyl urea and *N*-(*m*-tolyl) urea B-region analogues, **41** and **42**, which were nitrogen congeners of the α-carbon in **1** and **2**. Both proved to show only weak binding affinity. Additionally, **42** was unusual in that it failed under our standard assay conditions to show functional activity, either as an antagonist or as an agonist. This failure was traced to a slow unset of action, presumably due to slow penetration into the cells. If the *h*TRPV1-expressing CHO cells were incubated with **42** for 15 min before challenge with capsaicin, then full antagonism was observed with $K_{i(ant)}$ = 2200 nM. A further enhancement in antagonistic potency ($K_{i(ant)}$ = 860 nM) was observed if the pre-incubation time was extended to 30 min.

Using our human TRPV1 (*h*TRPV1) model[12] built based on our rat TRPV1 (rTRPV1) model[10], we performed a flexible docking study to investigate the binding interactions of compound **27**.[22] Compared with the lead compound **1*S***, compound **27** has a urea group in the B-region and an additional methylene group in the A-region. As shown in Figure 2, the binding mode of **27** was generally similar to that of **1*S***.[12] The urea group in the B-region was able to form a hydrogen bond with Tyr511 and also contributed to the appropriate positioning of A- and C-regions for the hydrophobic interactions. The *N*-benzylmethanesulfonamide group in the A-region occupied the deep bottom hole and

formed hydrophobic interactions with Tyr511, Tyr554, Ile564, and Ile569. The fluorine atom in the A-region made hydrogen bonds with Lys571 and the S═O of the sulfonamide group participated in hydrogen bonding with Ser512. The 3-trifluoromethyl group in the C-region extended toward the hydrophobic area composed of Leu547 and Thr550. Finally, the 4-methylpiperidine ring in the C-region was involved in the hydrophobic interactions with Tyr511, Met514, and Leu515.

In summary, we have investigated a series of homologated analogues of prototype antagonist **1** and its urea B-region surrogate as *h*TRPV1 ligands. From systematic one-carbon elongation in respective pharmacophoric regions, we identified *N*-(3-fluoro-4-methylsulfonamidomethylphenyl)urea, a one-carbon elongated analogue of the A-region in the urea B-region series, as a novel and potent TRPV1 antagonistic template. Its representative compound **27** showed high affinity and potent antagonism with K_i = 6.77 nM and $K_{i(ant)}$ = 12.5 nM which was comparable to that of **1**. Since the B-region of compound **27** is achiral urea unlike the chiral propanamide of **1**, it has more synthetic accessibility for further optimization and development. Docking analysis of compound **27** in our *h*TRPV1 homology model indicated that its binding mode was similar with that of **1*S*** previously reported.

Acknowledgments

This work was supported by the Korea Science and Engineering Foundation (KOSEF) grant funded by the Korea government (MOST) (NRF-2014M3A9B5073755), National Leading Research Lab (NLRL) program (2011-0028885), National Natural Science Foundation of China (81502927), Liaoning S&T Project (2014226032, 2015020733 and 2015001002), Hainan S&T Project (KYYS-2014-66), and in part by the Intramural Research Program of the NIH, Center for Cancer Research, NCI (Project Z1A BC 005270) in the USA.

References and notes

1. Szallasi A; Blumberg PM Pharmacol. Rev 1999, 51, 159. [PubMed: 10353985]
2. Tominaga M; Caterina MJ; Malmberg AB; Rosen TA; Gilbert H; Skinner K; Raumann BE; Basbaum AI; Julius D Neuron 1998, 21, 531. [PubMed: 9768840]
3. Szallasi A Am. J. Clin. Pathol 2002, 118, 110. [PubMed: 12109845]
4. (a)Walpole CS; Wrigglesworth R; Bevan S; Campbell EA; Dray A; James IF; Perins MN; Reid DJ; Winter J J. Med. Chem 1993, 36, 2362 [PubMed: 8360881] (b)Walpole CS; Wrigglesworth R; Bevan S; Campbell EA; Dray A; James IF; Masdin KJ; Perkins MN; Winter J J. Med. Chem 1993, 36, 2373 [PubMed: 8360882] (c)Walpole CS; Wrigglesworth R; Bevan S; Campbell EA; Dray A; James IF; Masdin KJ; Perkins MN; Winter J J. Med. Chem 1993, 36, 2381. [PubMed: 8360883]
5. Appendino G; Szallasi A Life Sci 1997, 60, 681. [PubMed: 9064473]
6. Min KH; Suh Y-G; Park M-K; Park H-G; Park Y-H; Kim H-D; Oh U; Blumberg PM; Lee J [published erratum appears in *Mol. Pharmacol.***2003**, *63*, 958] Mol. Pharmacol 2002, 62, 947. [PubMed: 12237342]
7. (a)Kym PR; Kort ME; Hutchins CW Biochem. Pharmacol 2009, 78, 211 [PubMed: 19481638] (b)Wong GY; Gavva NR Brain Res. Rev 2009, 60, 267 [PubMed: 19150372] (c)Gunthorpe MJ; Chizh BA Drug Discovery Today 2009, 14, 56 [PubMed: 19063991] (d)Lazar J; Gharat L; Khairathkar-Joshi N; Blumberg PM; Szallasi A Expert Opin. Drug Discovery 2009, 4, 159(e)Voight EA; Kort ME Expert Opin. Ther. Pat 2010, 20, 1 [PubMed: 20021282] (f)Szolcsányi J; Sándor Z Trend Pharmacol. Sci 2012, 33, 646(g)Szallasi A; Sheta M Expert Opin. Invest. Drug 2012, 21, 1351(h)De Petrocellis L; Moriello AS Recent Pat. CNS Drug Disc 2013, 8, 180(i)Lee Y; Hong S; Cui M; Sharma PK; Lee J; Choi S Expert Opin. Ther. Pat 2015, 25, 291. [PubMed: 25666693]
8. Liao M; Cao E; Julius D; Cheng Y Nature 2013, 504, 107. [PubMed: 24305160]

9. Cao E; Liao M; Cheng Y; Julius D Nature 2013, 504, 113. [PubMed: 24305161]
10. Lee JH; Lee Y; Ryu H; Kang DW; Lee J; Lazar J; Pearce LV; Pavlyukovets VA; Blumberg PM; Choi S J. Comput. Aided Mol. Des 2011, 25, 317. [PubMed: 21448716]
11. Feng Z; Pearce LV; Xu X; Yang X; Yang P; Blumberg PM; Xie XQ J. Chem. Inf. Model 2015, 55, 572. [PubMed: 25642729]
12. Kim MS; Ryu H; Kang DW; Cho S-H; Seo S; Park YS; Kim M-Y; Kwak EJ; Kim YS; Bhondwe RS; Kim HS; Park S-G; Son K; Choi S; DeAndrea-Lazarus I; Pearce LV; Blumberg PM; Frank R; Bahrenberg G; Stockhausen H; Kögel BY; Schiene K; Christoph T; Lee J J. Med. Chem 2012, 55, 8392. [PubMed: 22957803]
13. Thorat SA; Kang DW; Ryu H; Kim MS; Kim HS; Ann J; Ha T-H; Kim SE; Son K; Choi S; Blumberg PM; Frank R; Bahrenberg G; Schiene K; Christoph T; Lee J Eur. J. Med. Chem 2013, 64, 589. [PubMed: 23685943]
14. Ha T-H; Ryu H; Kim S-E; Kim HS; Ann J; Tran P-T; Hoang V-H; Son K; Cui M; Choi S; Blumberg PM; Frank R; Bahrenberg G; Schiene K; Christoph T; Frormann S; Lee J Bioorg. Med. Chem 2013, 21, 6657. [PubMed: 24035514]
15. Ryu H; Seo S; Cho S-H; Kim HS; Jung A; Kang DW; Son K; Cui M; Hong S-H; Sharma PK; Choi S; Blumberg PM; Frank-Foltyn R; Bahrenberg G; Stockhausen H; Schiene K; Christoph T; Frormann S; Lee J Bioorg. Med. Chem. Lett 2014, 24, 4039. [PubMed: 24948568]
16. Ryu H; Seo S; Cho S-H; Kim MS; Kim M-Y; Kim HS; Ann J; Tran P-T; Hoang V-H; Byun J; Cui M; Son K; Sharma PK; Choi S; Blumberg PM; Frank-Foltyn R; Bahrenberg G; Koegel B-Y; Christoph T; Frormann S; Lee J Bioorg. Med. Chem. Lett 2014, 24, 4044. [PubMed: 25011915]
17. Ryu H; Seo S; Lee J-Y; Ha T-H; Lee S; Jung A; Ann J; Kim S-E; Yoon S; Hong M; Blumberg PM; Frank-Foltyn R; Bahrenberg G; Schiene K; Stockhausen H; Christoph T; Frormann S; Lee J Eur. J. Med. Chem 2015, 93, 101. [PubMed: 25659771]
18. Tran P-T; Kim HS; Ann J; Kim S-E; Kim C; Hong M; Hoang V-H; Ngo VTH; Hong S; Cui M; Choi S; Blumberg PM; Frank-Foltyn R; Bahrenberg G; Stockhausen H; Christoph T; Lee J Bioorg. Med. Chem. Lett 2015, 25, 2326. [PubMed: 25937016]
19. Ann J;Jung A; Kim M-Y; Kim H-M; Ryu H; Kim S; Kang DW; Hong S; Cui M; Choi S; Blumberg PM; Frank-Foltyn R; Bahrenberg G; Stockhausen H; Christoph T; Lee J Bioorg. Med. Chem 2015, 23, 6844. [PubMed: 26474664]
20. Durandetti M; Nédélec J-Y; Périchon J J. Org. Chem 1996, 61, 1748. [PubMed: 11667045]
21. Veghel DV; Cleynhens J; Pearce LV; Blumberg PM; Laere KV; Verbruggen A; Bormans G Nucl. Med. Biol 2013, 40, 141. [PubMed: 23141549]
22. The 3D structures of the ligands were generated with Concord and energy minimized with MMFF94s force field and MMFF94 charge until the rms of Powell gradient was 0.05 kcal mol^{-1} A^{-1} in SYBYL-X 2.0 (Tripos Int., St. Louis, MO, USA). The flexible docking study on our *h*TRPV1 model was performed using GOLD v.5.2 (Cambridge Crystallographic Data Centre, Cambridge, UK), which employees a genetic algorithm (GA) and allows for full ligand flexibility and partial protein flexibility. The binding site was defined as 8 Å around the capsaicin complexed in the *h*TRPV1 model. The side chains of the nine residues which are important for ligand binding, (i.e., Tyr511, Ser512, Met514, Leu515, Leu518, Phe543, Leu547, Thr550, and Asn551) were allowed to be flexible with 'crystal mode' in GOLD. Compound **27** was docked using the GoldScore scoring function, and the other parameters remained as default. All the computation calculations were undertaken on an Intel® Xeon™ Quad-core 2.5 GHz workstation with Linux Cent OS release 5.5.

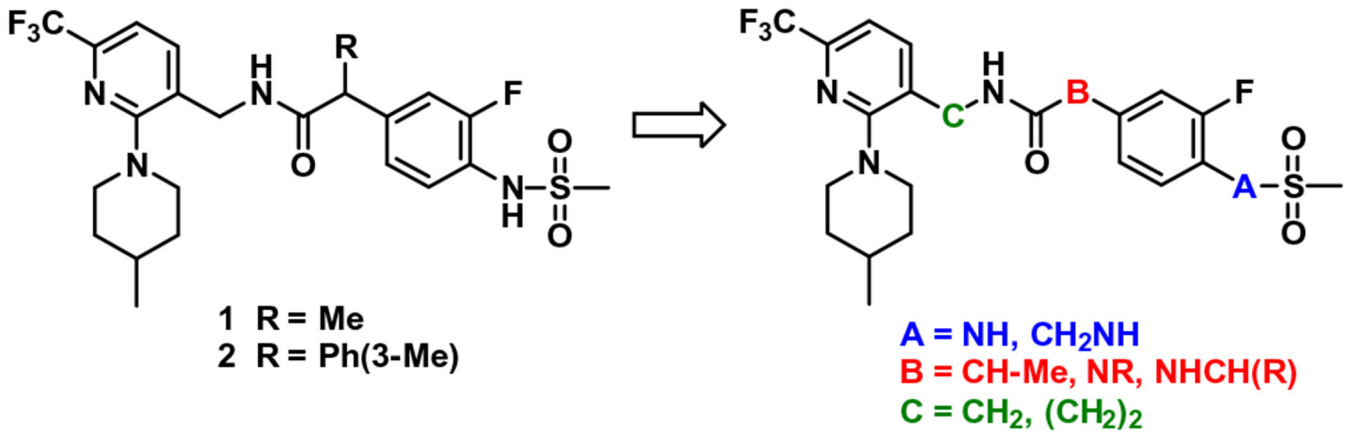

Figure 1.
Design of homologated congeners of prototype **1** as a TRPV1 antagonistic template.

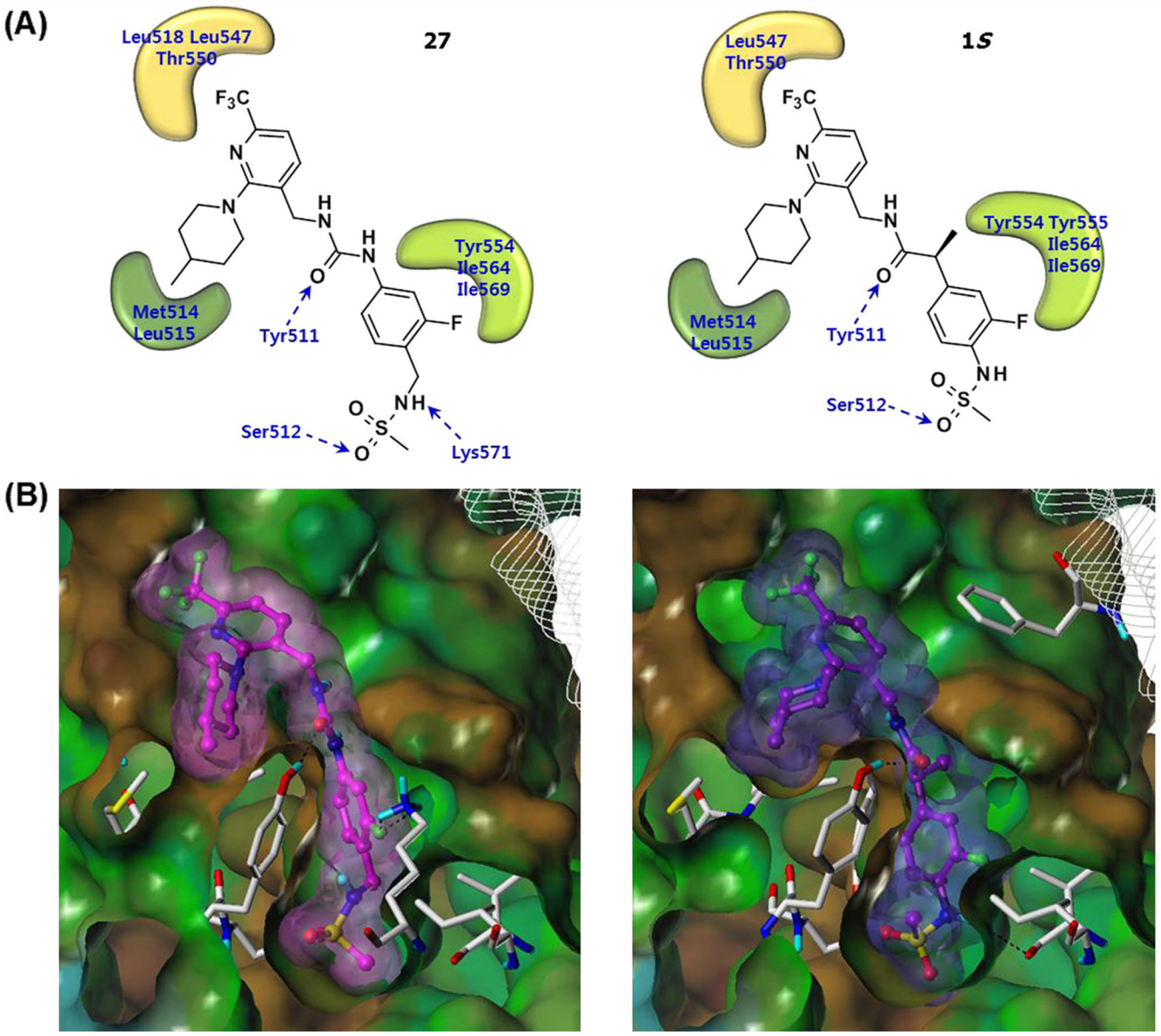

Figure 2.

Docking results of **27** and **1*S*** in the *h*TRPV1 model. (A) 2-D illustration of the binding interactions between **27** (left) and **1*S*** (right) with *h*TRPV1. Hydrogen bonding interactions are indicated by blue dashed line arrows and hydrophobic interactions are displayed with curved patches. (B) The Fast Connolly surface of *h*TRPV1 and the van der Waals surface of **27** (left) and **1*S*** (right). The molecular surface of *h*TRPV1 is created by using MOLCAD and presented with the lipophilic potential property. For clarity, the surface of *h*TRPV1 is Z-clipped and that of the ligands are colored individually by magenta (**27**) or purple (**1*S***).

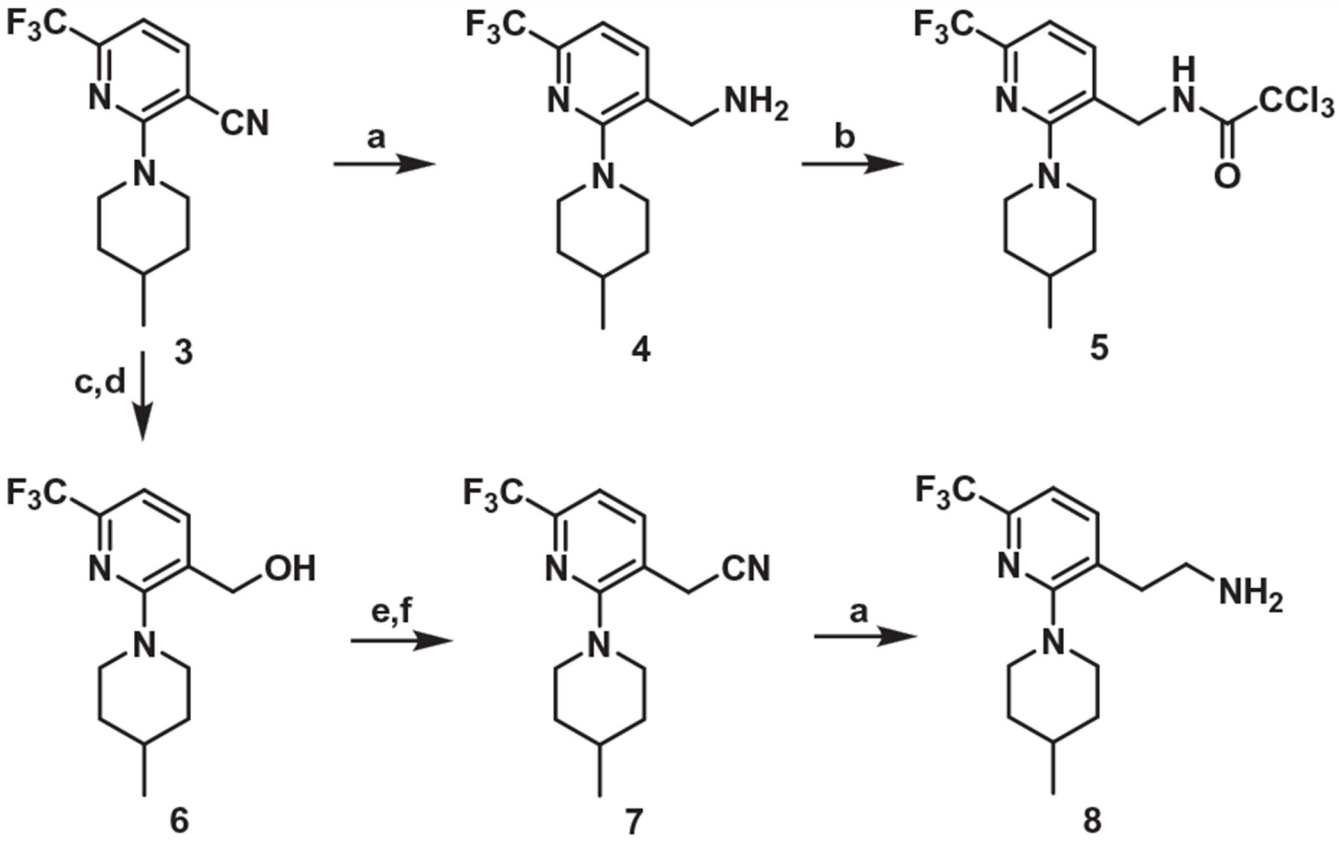

Scheme 1.

Synthesis of the C-region. Reagents and conditions: (a) $BH_3{\cdot}SMe_2$, THF, reflux, 3 h; (b) Cl_3CCOCl, TEA, CH_2Cl_2, rt, 3 h; (c) KOH, 80% aq EtOH, rt, 12 h (d) $LiAlH_4$, THF, rt, 14 h; (e) PBr_3, CH_2Cl_2, rt, 3 h; (f) KCN, EtOH, reflux, 8 h.

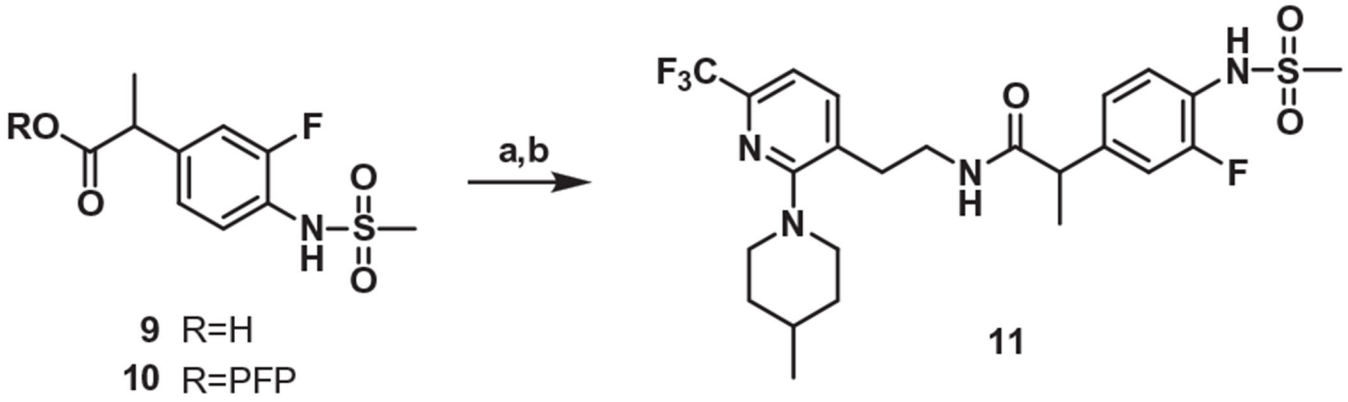

Scheme 2.

Synthesis of the propanamide B-region analog (One-carbon elongated C-region). Reagents and conditions: (a) pentafluorophenol, EDC, DMF, CH_2Cl_2; (b) compound **8**, TEA, CH_2Cl_2.

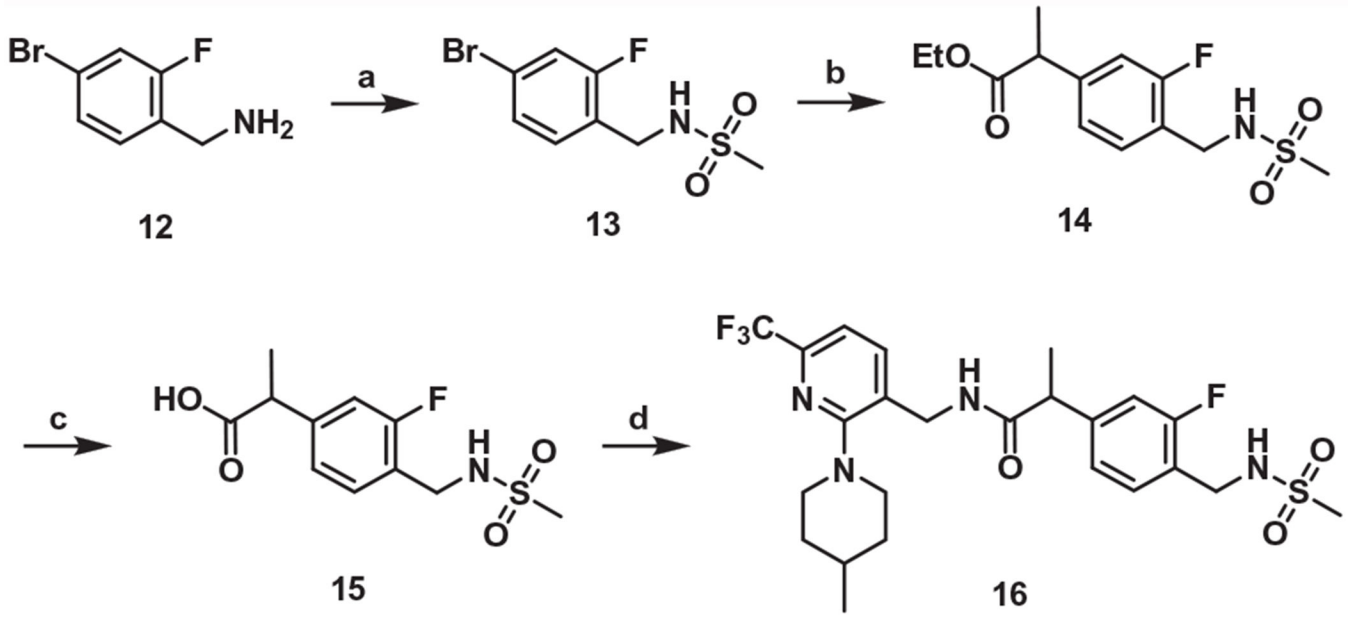

Scheme 3.

Synthesis of the propanamide B-region analog (One-carbon elongated A-region). Reagents and conditions: (a) MsCl, pyridine, 0 °C to rt, 2 h; (b) ethyl-2-chloropropionate, $NiBr_2(bpy)_2$, Mn, TFA, DMF, 65 °C, 15 h; (c) NaOH, THF/H_2O (1:1), 60 °C, 15 h; (d) compound **4**, EDC, HOBt, TEA, ACN, rt, 15

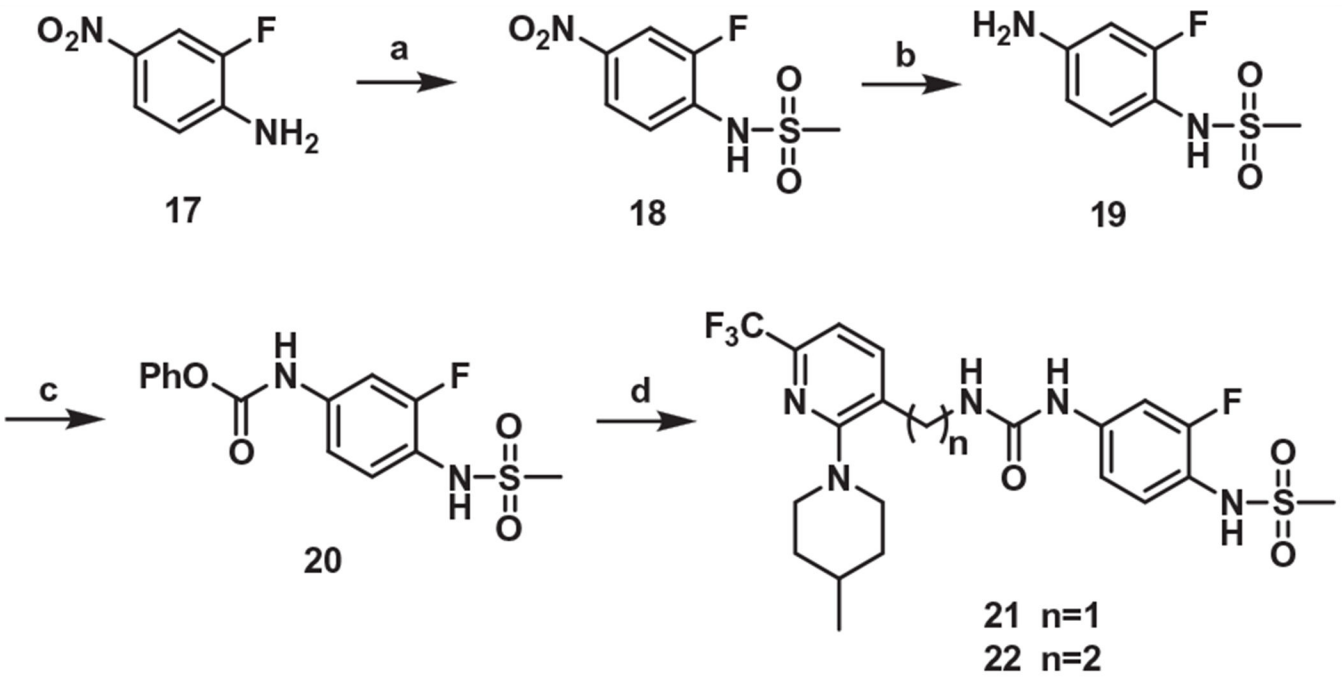

Scheme 4.

Synthesis of the urea B-region analog. Reagents and conditions: (a) MsCl, NaH, DMF, 0 °C → rt, 2h; (b) 10% Pd/C, H_2, CH_2Cl_2; (c) phenylchloroformate, pyridine, THF, 0 °C, 1 h; (d) compound **4** for **21**, compound **8** for **22**, DMAP, MeCN, 50 °C, 6 h.

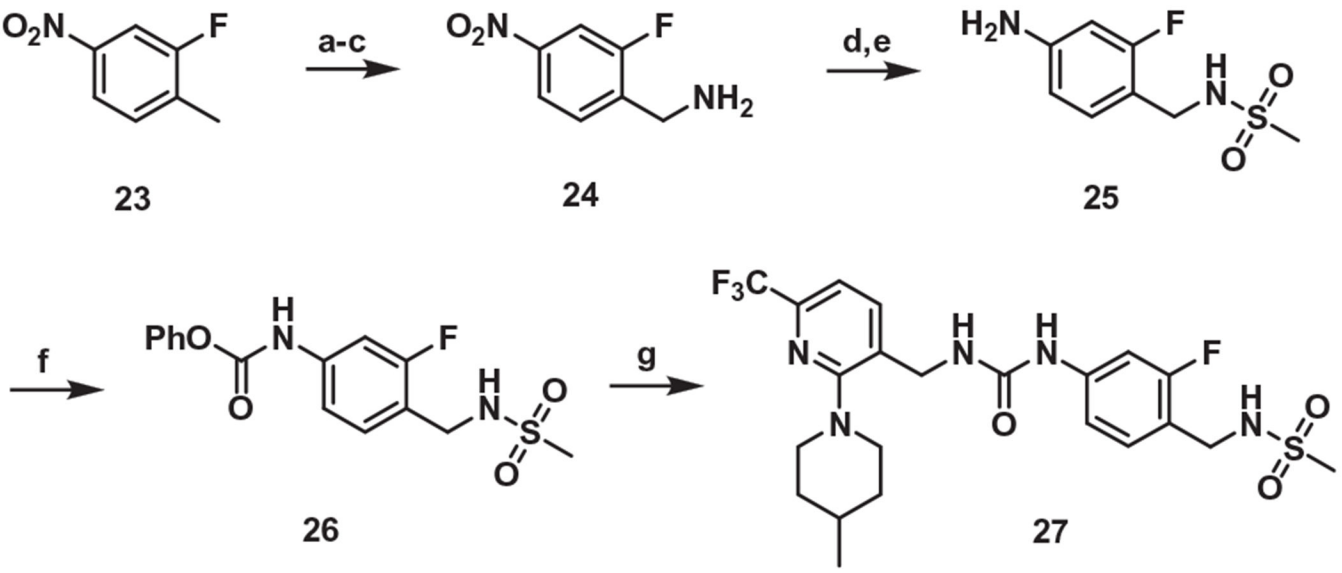

Scheme 5.

Synthesis of the urea B-region analog (One-carbon elongated A-region). Reagents and conditions: (a) benzoyl peroxide, NBS, CCl_4, reflux, 15h; (b) potassium phthalimide, DMF, r.t, 15h; (c) hydrazine monohydrate, PTSA, THF, reflux, 6 h; (d) MsCl, Pyridine, rt, 1 h; (e) 10% Pd/C, H_2 gas, THF/EtOH, rt, 15 h; (f) phenylchloroformate, pyridine, THF/CAN; (g) compound **4**, DMAP, MeCN, 50 °C, 6 h.

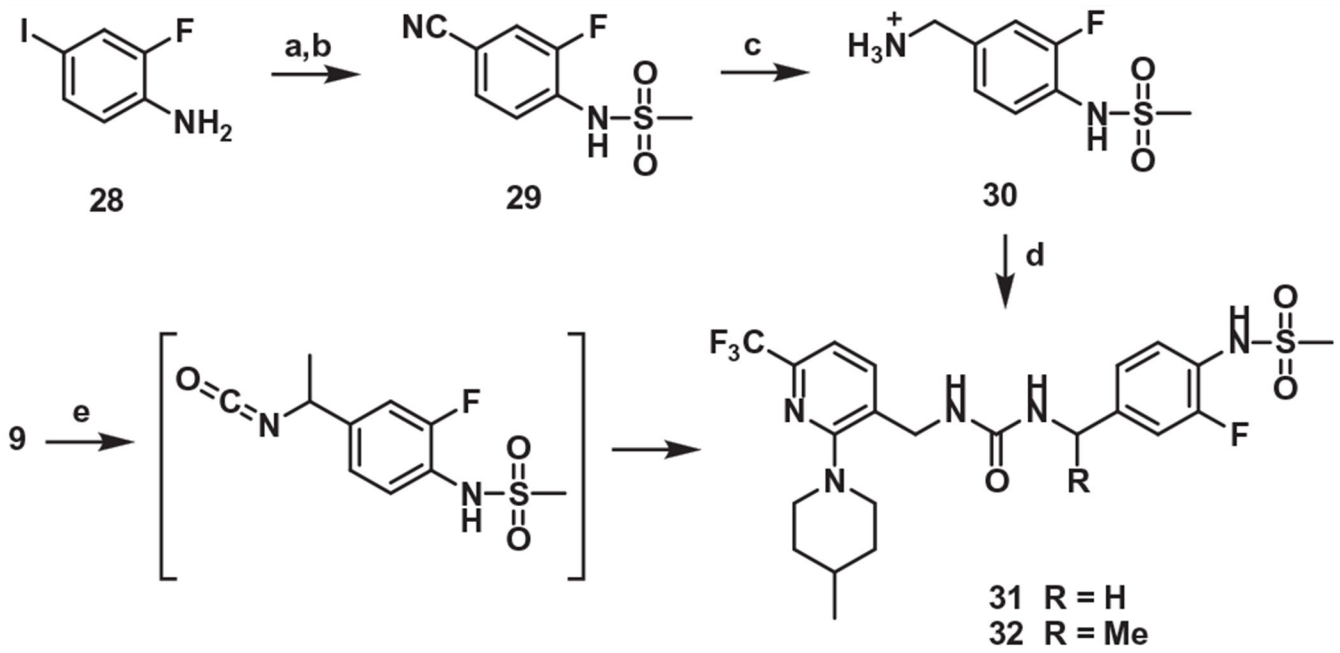

Scheme 6.

Synthesis of the urea B-region analog (One-carbon elongated B-region). Reagents and conditions: (a) MsCl, Pyridine, rt, 2 h; (b) $Zn(CN)_2$, $Pd(PPh_3)_4$, DMF, 150 °C, 15 h; (c) (i) 2 M $BH_3{\cdot}SMe_2$, THF, reflux, 3 h, (ii) 1 M HCl, reflux, 15 h; (d) compound **4**, DBU, DMF, 80 °C, 2h; (e) (i) DPPA, TEA, toluene, 110 °C, 1 h, (ii) compound **4**, 80 °C, 15h.

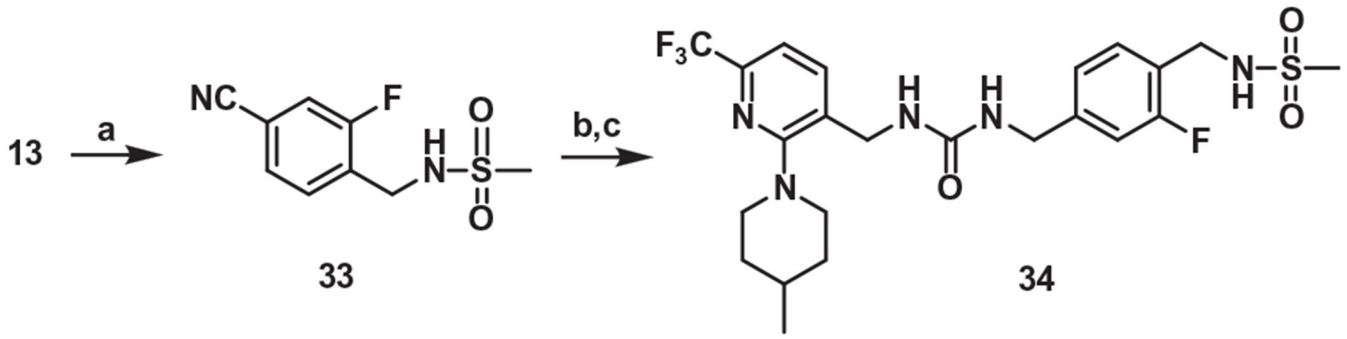

Scheme 7.

Synthesis of the urea B-region analog (One-carbon elongated A and B-region). Reagents and conditions: (a) $Zn(CN)_2$, Zn, $Pd_2(dba)_3$, dppf, DMA, sealed tube, 120 °C, 15 h; (b) 10% Pd/C, MeOH, H_2 gas, rt, 15 h; (c) compound **5**, DBU, DMF, 80 °C, 2 h.

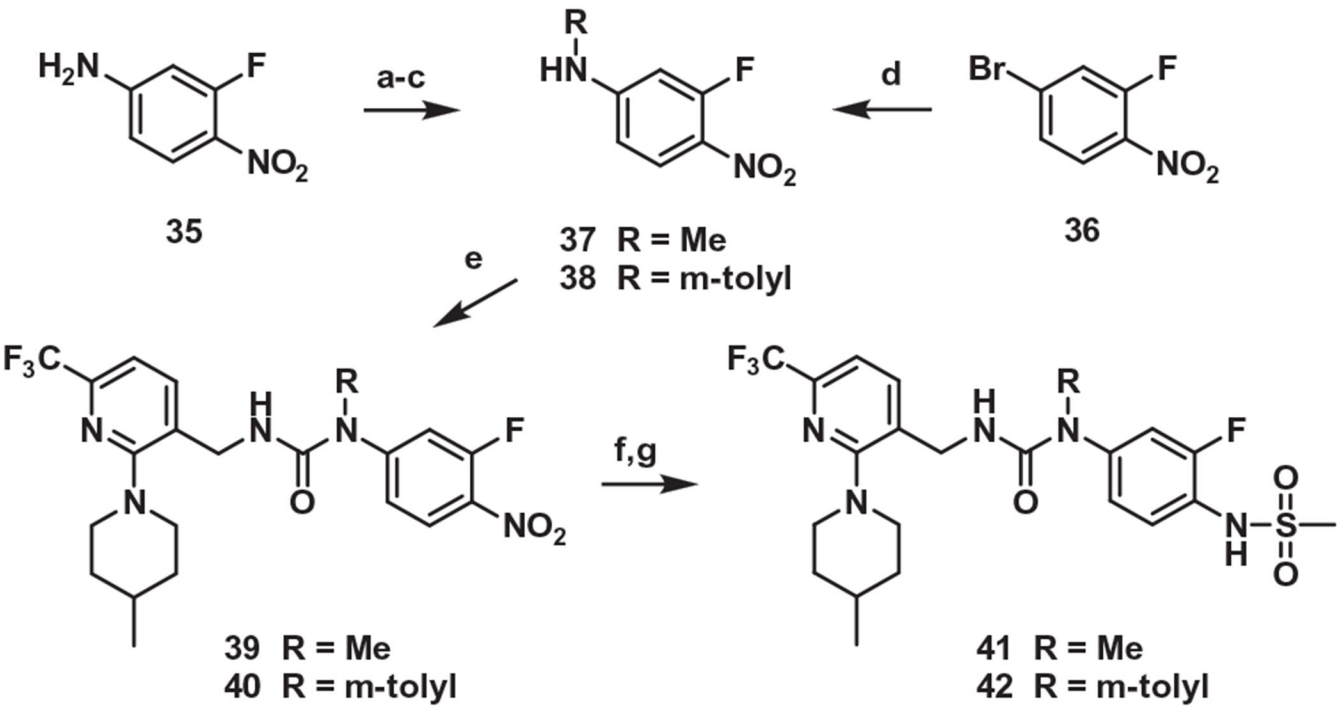

Scheme 8.

Synthesis of the urea B-region analog (*N*-methyl urea). Reagents and conditions: (a) Boc_2O, TEA, CH_2Cl_2, reflux,15 h; (b) Cs_2CO_3, CH_3I, DMF, 40 °C, 15 h; (c) TFA, CH_2Cl_2, 0 °C → rt, 2 h; (d) *m*-toluidine, $Pd(OAc)_2$, Xantphos, Cs_2CO_3, 1,4-dioxane, reflux,15 h; (e) (i) pyridine, triphosgene, toluene, rt, 2 h, (ii) compound **4**, TEA, CH_2Cl_2, rt, 15 h; (f) 10% Pd/C, H_2 gas, MeOH, rt → 40 °C, 30 min; (g) MsCl, pyridine, CH_2Cl_2, rt, 15 h.

Bioorg Med Chem Lett. Author manuscript; available in PMC 2020 January 13.

Table 1

In vitro activity of synthesized compounds on *h*TRPV1[a]

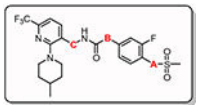

	A	B	C	Binding affinity K_i(nM)		Agonism EC_{50} (nM)	Antagonism $K_{i(ant)}$ (nM)	
1	–NH	CH–Me	CH_2	7.90	(±1.6)	NE	2.22	(±0.47)
1*S*	–NH	(*S*)-CH–Me	CH_2	2.95	(±0.73)	NE	1.26	(±0.28)
11	–NH	CH–Me	$(CH_2)_2$	54	(±13)	NE	95	(±26)
16	$–CH_2NH$	CH–Me	CH_2	230	(±32)	NE	27.6	(±5.5)
21	–NH	NH	CH_2	83	(±27)	NE	149	(±50)
22	–NH	NH	$(CH_2)_2$	210	(±46)	29%	49%	
27	$–CH_2NH$	NH	CH_2	6.77	(±0.48)	NE	12.5	(±4.2)
31	–NH	$NHCH_2–$	CH_2	59	(±12)	NE	18.7	(±6.1)
32	–NH	NHCH(Me)–	CH_2	31.6	(±3.4)	NE	28.1	(±8.5)
34	$–CH_2NH$	$NHCH_2–$	CH_2	410	(±27)	NE	199	(±50)
41	–NH	NH–Me	CH_2	1160	(±180)	NE	59	(±20)
42	–NH	NH–Ph(3-Me)	CH_2	490	(±120)	NE	860[b]	(±290)[b]

[a]NE: no effect; values are the mean ± SEM of at least three experiments; where indicated, % represents the % agonism or antagonism at 3–30 μM.

[b]Measured with 30 min pre-incubation before challenge with capsaicin; value with 15 min pre-incubation $K_{i(ant)}$ = 2200 ± 560 nM.